Plant Science 226 (2014) 49–60

Contents lists available at ScienceDirect

Plant Science

journal homepage: www.elsevier.com/locate/plantsci

Inconsistency of mesophyll conductance estimate causes the inconsistency for the estimates of maximum rate of Rubisco carboxylation among the linear, rectangular and non-rectangular hyperbola biochemical models of leaf photosynthesis—A case study of CO_2 enrichment and leaf aging effects in soybean

Jindong Sun[a,*], Zhaozhong Feng[a,1], Andrew D.B. Leakey[a,b], Xinguang Zhu[b,2], Carl J. Bernacchi[b,c], Donald R. Ort[a,b,c]

[a] Institute for Genomic Biology, University of Illinois at Urbana-Champaign, Urbana, IL 61801, USA
[b] Department of Plant Biology, University of Illinois at Urbana-Champaign, Urbana, IL 61801, USA
[c] Photosynthesis Research Unit, USDA-ARS, Urbana, IL 61801, USA

ARTICLE INFO

Article history:
Available online 27 June 2014

Keywords:
A/C_i curves
Mesophyll conductance
Maximum rates of carboxylation
Soybean
CO_2
Leaf age

ABSTRACT

The responses of CO_2 assimilation to [CO_2] (A/C_i) were investigated at two developmental stages (R5 and R6) and in several soybean cultivars grown under two levels of CO_2, the ambient level of 370 μbar versus the elevated level of 550 μbar. The A/C_i data were analyzed and compared by either the combined iterations or the separated iterations of the Rubisco-limited photosynthesis (A_c) and/or the RuBP-limited photosynthesis (A_j) using various curve-fitting methods: the linear 2-segment model; the non-rectangular hyperbola model; the rectangular hyperbola model; the constant rate of electron transport (J) method and the variable J method. Inconsistency was found among the various methods for the estimation of the maximum rate of carboxylation (V_{cmax}), the mitochondrial respiration rate in the light (Rd) and mesophyll conductance (g_m). The analysis showed that the inconsistency was due to inconsistent estimates of g_m values that decreased with an instantaneous increase in [CO_2], and varied with the transition C_i cut-off between Rubisco-limited photosynthesis and RuBP-regeneration-limited photosynthesis, and due to over-parameters for non-linear curve-fitting with g_m included. We proposed an alternate solution to A/C_i curve-fitting for estimates of V_{cmax}, Rd, J_{max} and g_m with the various A/C_i curve-fitting methods. The study indicated that down-regulation of photosynthetic capacity by elevated [CO_2] and leaf aging was due to partially the decrease in the maximum rates of carboxylation and partially the decrease in g_m. Mesophyll conductance lowered photosynthetic capacity by 18% on average for the case of soybean plants.

Abbreviations: A, net rate of CO_2 uptake per unit of projected leaf area; A_c, Rubisco-limited photosynthesis; A_j, RuBPlimited photosynthesis; α, leaf absorbance; ANOVA, analysis of variance; C_i, intercellular CO_2 concentration; C_c, CO_2 concentration at the chloroplast site; C_{itr}, the transition C_i between A_c and A_j; [CO_2], CO_2 concentration; CJ, constant J method; β, fraction of absorbed quanta of photons partitioning between incident PSII and PSI; FACE, free air CO_2 enrichment; F'_m, maximal yield of fluorescence from a saturating flash of white light; F_s, steady-state fluorescence; g_m, mesophyll conductance; g_{m1}, mesophyll conductance estimated from Rubisco-limited photosynthesis; g_{m2}, mesophyll conductance estimated from RuBP-limited photosynthesis; J, rate of electron transport; J_{max}, maximum rate of electron transport; K_c, Rubisco Michaelis constant for CO_2; K_o, Rubisco Michaelis constant for O_2; O, concentration of oxygen in air; PPFD, photosynthetic photon flux density; Rd, mitochondrial respiration rate in the light; TPU, triose-phosphate utilization; V_{cmax}, maximum rate of Rubisco carboxylation; VJ, variable J method; Γ^*, CO_2 compensation point in the absence of dark respiration; Φ_{PSII}, quantum yield of PSII.

* Corresponding author. Current address: DuPont Pioneer, Johnston, IA 50131, USA. Tel.: +1 515 535 4995; fax: +1 515 535 3444.
E-mail addresses: jindong.sun@pioneer.com, jindong.sun@gmail.com (J. Sun).
[1] Current address: State Key Laboratory of Urban and Regional Ecology, Research Center for Eco-Environmental Sciences, Chinese Academy of Sciences, Beijing 100085, China.
[2] Current address: CAS-MPG Partner Institute of Computational Biology, Shanghai 200031, China.

http://dx.doi.org/10.1016/j.plantsci.2014.06.015
0168-9452/

1. Introduction

Global climate change especially the rising CO_2 levels has fundamental effects on plant photosynthesis including important properties such as the maximum rates of Rubisco carboxylation (V_{cmax}) the maximum rates of electron transport (J_{max}) and the mitochondrial respiration rate in the light (Rd) [1,2]. Unbiased accurate estimates of V_{cmax}, J_{max} and Rd are getting more important and critical for predicting global climate change impacts.

V_{cmax}, J_{max} and Rd can be analyzed by responses of CO_2 assimilation to C_i, i.e. A/C_i curves using the well accepted biochemical models of Farquhar's [3] and the derivatives [4–6]. A variety of methods have been used to estimate V_{cmax}, J_{max} and Rd based on A/C_i responses [3,4,6–12]. The widely used method is to solve V_{cmax}, J_{max} and Rd using the least square fitting of linear model by simply replacing C_c, the [CO_2] at the chloroplast site, with C_i, the intercellular [CO_2] [*e.g.* 6,9]. Basically, the transition C_i was estimated by looking at the relatively linear part of an A/C_i curve and/or based on literature information, and the R square value was used to justify the best linear fit. Often the assumed C_i value based on some of the previous literature is unreliable.

There is increasing evidence that mesophyll conductance (g_m), the intercellular CO_2 transfer conductance, may impose significant limitation to photosynthesis and affect A/C_i responses [8,13–15]. V_{cmax} would be underestimated when g_m is low and not accounted for. The g_m can be estimated by the combined chlorophyll fluorescence with gas exchange [7,8], and the isotope method [16]. There is a good agreement between these two methods [15].

It has been proposed that g_m can also be estimated by using the least square fitting of non-rectangular model [13,14] and by using the least square fitting of rectangular model [11]. Various versions of the Farquhar's models [3,9,11,13,14] add complexity and variations. In addition, the photosynthetic properties can be estimated from the Farquhar's model using the Rubisco limited photosynthesis equation and the RuBP-limited photosynthesis equation either through separated fitting of each of the two equations [6,9] or through the combined iterations of the two equations together [10,11]. Direct comparisons of various curve fitting methods using a large set of real experimental data with various treatments are still rare and yet important. The inconsistency among various curing fitting methods was found (Jindong Sun et al., abstract #P03008, ASPB, 2008). A study discussing the comparisons of some non-linear methods has been reported [12]. A constant 20 Pa [CO_2] was used as the transition C_i between Rubisco and RuBP-limited photosynthesis for 4 of the 6 methods for comparisons and the linear method was not included [12]. It is concluded that the rectangular method [11] was better than other methods [12].

In the present study, we compared the photosynthetic parameters, V_{cmax}, J_{max}, Rd and g_m, by either the combined iterations or the separated iterations of Rubisco-limited and RuBP-limited photosynthesis using various methods of the linear, rectangular and non-rectangular models [7,9–11,14] using A/C_i data only. We investigated the effects of long-term [CO_2] enrichment (550 μbar versus 370 μbar) and leaf aging (R6 versus R5 stages) on the responses of CO_2 assimilation to [CO_2] and leaf chlorophyll fluorescence in naturally field-grown soybean in SoyFACE. We compared various curve-fitting methods and proposed a solution to A/C_i curve-fitting. We developed a program with Excel macro and SAS code with which the whole A/C_i curve was accounted for estimates of V_{cmax} and J_{max}, R_d and g_m and for convenient and high throughput analysis of large amount of data with A/C_i curves only.

2. Materials and methods

2.1. Plant material and SoyFACE design

The study was conducted at the SoyFACE facility (Champaign, IL). The field was managed according to standard regional agronomic practice for annual corn/soybean rotation. SoyFACE was designed with 4 blocks of paired rings (ambient and elevated). Each ring contained 20-m diameter octagonal plots. The control rings were at current ambient [CO_2] of 370 μbar (C370) and the elevated CO_2 rings were fumigated from sunrise to sunset to an elevated target [CO_2] of 550 μbar (C550). Eleven soybean cultivars [*Glycine max* (L.) Merr.] were planted in 0.38 m rows in each block. Four cultivars cv. A3127, Clark and IA3010 and 93B15 were sampled at late R5 stage (DOY 230) when no visible senescence occurred and late R6 stage (DOY 245) when visible senescence occurred in 2007 for the following measurements. Two or three fully expanded young leaves were selected at random for each cultivar in each block for gas exchange and the remaining measurements, respectively. A total of 128 samples were measured for A/C_i responses by gas exchange and chlorophyll fluorescence.

2.2. Gas exchange

Gas exchange was measured using four portable gas exchange systems (LI-COR 6400LCF; LI-COR, Lincoln, NE) following the procedure described in [9]. The CO_2 sensors and water vapor sensors of the gas exchange systems were calibrated using gas of a known [CO_2] with 21% oxygen and nitrogen as balance, and known water vapor concentrations generated with a controlled humidification system, respectively (LI-610 Portable Dew Point Generator; LI-COR). Leaf temperatures were set at 25 °C, and PPFD levels were maintained at 1500 μmol m^{-2} s^{-1} using a chamber integrated red-blue light source with 10% blue light for all of the measurements. The relative humidity was maintained between 60 and 70% in the leaf chamber. After steady-state CO_2 and water vapor exchange were achieved measurements of A were made starting at 400 μbar [CO_2] surrounding the leaf, and [CO_2] was decreased stepwise to 50 μbar [CO_2]. The [CO_2] was then set again to 400 μbar and increased stepwise to 1500 μbar. Each individual A/C_i curve consisted of 11 individual measurements at various [CO_2] levels (400, 200, 100, 50, 400, 600, 800, 1000, 1200 and 1500 μbar) and took approximately 40 min to complete. We chose the 10 CO_2 levels because more CO_2 data points would add more time and work, but would not gain significantly better resolutions or affect the conclusions. Leaks to CO_2 diffusion had been considered and corrected based on the CO_2 gradients and flow rate as described (Licor 6400 manual, Licor, Inc., Lincoln, NE). We used high flow rate (500 μmol per second) to further reduce diffusion effect.

2.3. Chlorophyll fluorescence

Chlorophyll fluorescence was measured simultaneously with gas exchange (see gas exchange) using four portable gas exchange systems with the integrated chlorophyll fluorescence chamber (LI-6400LCF, LI-COR, Lincoln, NE). Φ_{PSII} was calculated as $(F'_m - F_s)/F'_m$ and ETR was calculated as $(\Phi_{PSII} \times PPFD \times \alpha \times \beta)$ [17], where α, the light absorbed by the leaf, was assumed to be 0.85 [16], and β, the factor for the partitioning of photons between incident PSII and PSI, was assumed to be 0.5 [18]. We used absorbance 0.85 because we used light source consisted of 90% red light and 10% blue light and the red and blue light absorbances were around 0.83 and 0.91, respectively, for beans (Licor manual, Licor, Inc., Lincoln, NE).

2.4. A/C_i curve fitting

The maximum carboxylation capacity (V_{cmax}), the maximum capacity for electron transport rate (J_{max}) and mitochondrial respiration in the light (Rd) for A/C_i curves were calculated using the equations of von Caemmerer and Farquhar [4], and using the temperature dependent kinetic parameters of Rubisco described on a C_c basis by Bernacchi et al. [19]. Raw data that were below the transition between Rubisco- and RuBP regeneration-limited photosynthesis were fit using the equations representing Rubisco-limited A (A_c).

$$A_c = \frac{V_{cmax}(C_c - \Gamma^*)}{(C_c + K_c(1 + O/K_o))} - Rd \quad (1)$$

Raw data located above the transition were fit using the equations representing RuBP regeneration-limited A (A_j)

$$A_j = \frac{J(C_c - \Gamma^*)}{(4C_c + 8\Gamma^*)} - Rd \quad (2)$$

And the relationship between C_c and C_i is as following:

$$C_c = C_i - \frac{A}{g_m} \quad (3)$$

In some cases, there was another transition called TPU-limited A when further increases in C_i resulted in a plateau or slight decreases in A with an additional increase in C_i ($dA/dC_i < 0$) if triose-phosphate utilization (TPU) becomes limiting [5,6]. When A is limited by TPU, the simple form is the following:

$$A = 3\ \mathrm{TPU} - Rd \quad (4)$$

Putting aside the TPU-limited photosynthesis, Eqs. (1)–(3) have four parameters that need to be solved, i.e. V_{cmax}, J_{max}, Rd and g_m.

2.5. Solution method 1s (M1s)

Replacing C_c with C_i, in Eqs. (1) and (2) and using K_c, K_o and Γ^* as a *priori*, V_{cmax}, J_{max} and Rd were determined from each A/C_i curves using linear least square fit with Rd as the intercept and V_{cmax} and J_{max} as the slopes using Eqs. (1) and (2), respectively [9]. The apparent Rubisco constant formula used for fitting, $K_c(1 + O/K_o)$, is independent of CO_2 and O_2 levels [21]. Rd was solved from Eq. (1) and used for Eq. (2) as a *priori*. In this method the Rubisco-limited and RuBP-limited portions of A/C_i responses were analyzed separately by linear least square fit.

2.6. Solution method 1c (M1c)

Replacing C_c with C_i in Eqs. (1) and (2), and using K_c, K_o and Γ^* as a *priori*, V_{cmax}, J_{max} and Rd were determined from each A/C_i curves by combined iterations of both Eqs. (1) and (2) using 2-segment linear least square fit, rather than treating the least square fits of the Rubisco-limited and RuBP-limited A/C_i portions separately.

2.7. Solution method 2c (M2c)

Using K_c, K_o and Γ^* as a *priori*, V_{cmax}, J_{max} and Rd as well as g_m were determined from each A/C_i curves by combined iterations using non-linear least square fit of the rectangular hyperbola curve with Eqs. (1)–(3). The excel macro of Sharkey et al. was used for the iterations using Eqs. (1)–(3) to solve the 4 parameters, i.e. V_{cmax}, J_{max}, Rd and g_m [11].

2.8. Solution method 2s (M2s)

Using K_c, K_o and Γ^* as a *priori*, V_{cmax}, Rd as well as g_{m1} were determined from the Rubisco-limited portion of each A/C_i curves by iterations using non-linear least square fit with Eq. (1), and J_{max} and g_{m2} were determined from the RuBP-limited portion of each A/C_i curves by iterations using non-linear least square fit with Eq. (2) with Rd fixed from the Eq. (1). Root mean square errors (RMSE) were used to fit to find the transition point. In this method the Rubisco-limited and RuBP-limited portions of A/C_i responses were analyzed separately by non-linear least square fit of the rectangular hyperbola curve.

2.9. Solution method 4s (M4s)

Ethier et al. [13,14] used a non-rectangular hyperbola version of the biochemical model of C3 leaf photosynthesis of Farquhar et al. [3,6] that accounts for g_m and whereby the solutions of A_c and A_j are given as

$$A_c = \frac{-b + \sqrt{b^2 - 4ac}}{2a} \quad (5)$$

where $a = -1/g_{m1}$, $b = (V_{c\max} - Rd)/g_{m1} + C_i + K_c(1 + O/K_o)$ and $c = Rd(C_i + K_c(1 + O/K_o)) - V_{c\max}(C_i - \Gamma^*)$.

$$A_j = \frac{-b + \sqrt{b^2 - 4ac}}{2a} \quad (6)$$

where $a = -1/g_{m2}$, $b = (J/4 - Rd)/g_{m2} + C_i + 2\Gamma^*$ and $c = Rd(C_i + 2\Gamma^*) - J/4(C_i - \Gamma^*)$.

Using K_c, K_o, Γ^* as a *priori*, V_{cmax}, Rd and g_{m1} were determined by fitting Eq. (5) to the data for the Rubisco-limited A/C_i portions by iterations, and J_{max} and g_{m2} were determined by fitting Eq. (6) to the data for RuBP-limited A/C_i portions by iterations with Rd fixed as a *priori* from calculation of Eq. (5). Root mean square errors (RMSE) were used to fit to find the transition point. In this method the Rubisco-limited and RuBP-limited portions of A/C_i responses were analyzed separately by non-linear least square fit of the non-rectangular hyperbola curve.

2.10. Solution method 4c (M4c)

Using K_c, K_o, Γ^* as a *priori*, V_{cmax}, J_{max}, Rd and g_m were determined from the above Eqs. (5) and (6) from each A/C_i curves using non-linear least square fit of the non-rectangular hyperbola curve by combined iterations to obtain a unique estimate for g_m, i.e. g_{m1} equals g_{m2}.

2.11. The transition C_i (C_{itr})

For each A/C_i response curve, the transition in which photosynthetic control moves from being Rubisco- to RuBP regeneration-limited was calculated based on the values of Rd, V_{cmax} and J_{max} as well as g_m if applied from the curve fitting. The transition C_i was found where the Rubisco-limited photosynthesis equaled RuBP-limited photosynthesis (i.e. $A_c = A_j$, A_c and $A_j > 0$, von Caemmerer [6]).

2.12. Curve fitting

Since several methods were used to solve several parameters using various equations (Eqs. (1)–(7)), the calculations were time consuming. In this study, we created computing programs using Excel visual basic macro with solver function and SAS code (see Supplemental materials) to estimate V_{cmax}, J_{max}, Rd as well as g_m and C_{itr} using various methods by least square fitting (root-mean-square-errors) of each of the A/C_i curves. The calculated A was set as the minimum A_c and A_j to fit the A/C_i curves for various methods (Eq. (7)). C_{itr} was determined automatically by the program, and multiple data sets of A/C_i curves were processed in a high through-put

way using Excel macro or SAS code to improve the efficiency and accuracy. There are good correlations for the estimates between Excel macro and SAS code.

$$A = \min(A_c, A_j) \tag{7}$$

2.13. Estimation of mesophyll conductance by constant J and variable J methods

g_m for each of the A/C_i curves were calculated by both the constant J method and the variable J method [7] and using the values of Γ^* at a given temperature from [20]. The g_m was constrained to 30 since a wide range of g_m values could satisfy the equations when it was large to infinite [7]. For variable J methods g_m was solved by the following equation using A, C_i and Rd measured from gas exchange (Rd was calculated by fitting A/C_i data, which generally agreed with measured Rd, data not shown), and rates of electron transport, J, measured using chlorophyll fluorescence. C_i between 100 and 300 μbar was used for the g_m calculation as lower variations occurs inside this range [7]. Though there are some limitations for variable J method as in other methods [22], variable J method uses chlorophyll fluorescence to estimate g_m which is different from gas exchange A/C_i fitting, and would be good alternate proof. It does not mean that the variable J method is invalid itself, rather, it is suggested that variable J method should not be used to study the point responses of g_m to environmental variations in an instantaneous mode [22]. Our study was mainly focused on responses of g_m to chronic elevated CO_2 enrichment and leaf development (age), rather than instantaneous changes.

$$g_m = \frac{A}{C_i - (\Gamma^*(J + 8(A + Rd))/(J - 4(A + Rd)))} \tag{8}$$

For the constant J methods g_m was solved by the following equation using A, C_i and Rd measured from gas exchange. This equation requires chlorophyll fluorescence measurements to determine the C_i range where J is constant and photosynthesis is RuBP regeneration-limited. Data were selected from CO_2-response measurements in the region where Φ_{PSII} was constant with increasing [CO_2].

$$J = (A + Rd)\frac{4((C_i - A/g_m) + 2\Gamma^*)}{(C_i - A/g_m) - \Gamma^*} \tag{9}$$

The values obtained for g_m were used to convert A–C_i curves into A–C_c curves and were compared with the g_m estimated from other methods.

After initial analysis, we found that g_m had huge variation and could be very large to infinite in many cases, and we restricted maximum g_m to 30 (as [11]) at which the g_m effect on photosynthesis is almost negligible in order to be able to compare the effects of [CO_2] and leaf aging on g_m.

2.14. Statistical analysis

All measured parameters influenced by [CO_2] treatments, developmental stages and cultivars were analyzed by use of SAS ANOVA and the means and standard errors were calculated by use of SAS MEANS (SAS System 9.1; SAS Institute, Cary, NC) Significant probability values were set at $p < 0.1$ to avoid type II error.

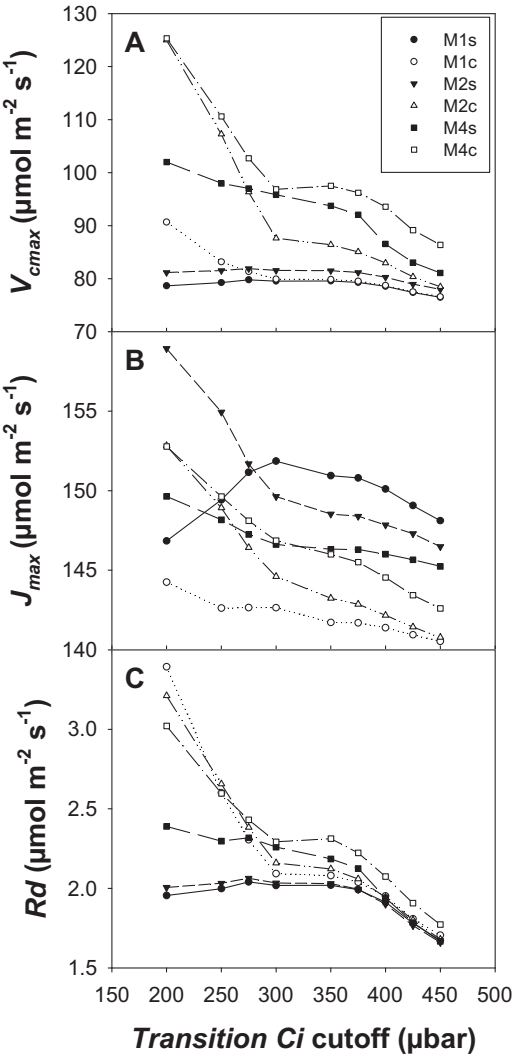

Fig. 1. Effects of transition C_i cut-off on V_{cmax}, J_{max} and Rd using various methods (● M1s, ○ M1c, ▼ M2s, ▽ M2c, ■ M4s and □ M4c). The estimates were the average across the whole set of data from SoyFACE.

3. Results

3.1. Effects of transition C_i cut-off on V_{cmax}, J_{max} and Rd and g_m estimated by various methods

3.1.1. Effects of the transition C_i cut-off on V_{cmax}, J_{max} and Rd

The effects of the transition C_i cut-off on the estimates of V_{cmax}, J_{max} and Rd were analyzed with various methods with the whole A/C_i data set from SoyFACE. The transition C_i had significant effects on estimates of V_{cmax}, J_{max} and Rd (Fig. 1). Transition C_i affected V_{cmax} and Rd on much higher degree than J_{max}. Within the range of transition C_i from 200 to 450 μbar, Rd varied from 1.7 to 3.4, V_{cmax} varied from 77 to 125, and J_{max} varied from 141 to 159 from method to method.

Different methods showed different patterns in response to transition C_i (Fig. 1). First, V_{cmax}, J_{max} and Rd decreased with increase in transition C_i for various methods. The differences of V_{cmax}, J_{max} and Rd among various methods were larger under lower transition C_i than under higher transition C_i. Second, the values of V_{cmax} and Rd estimated from the combined iteration methods (M4c, M2c and M1c) were higher than that estimated from the separated iteration methods (M4s, M2s and M1s). Third, the values of V_{cmax} and Rd

estimated from the non-rectangular hyperbola models (M4s and M4c) were higher than that estimated from the rectangular hyperbola models (M2s and M2c), which in turn was higher than that estimated from the linear models (M1s and M1c).

Regarding V_{cmax} and *Rd* estimates, the linear methods (M1s and M1c) were relatively less sensitive to transition C_i compared with the other non-linear methods, and the separated iteration methods were relatively less sensitive to transition C_i compared with the combined iteration methods (Fig. 1). V_{cmax} estimated by M1s changed little with various transition C_i. *Rd* estimated by M1s changed little with various transition C_i between 200 and 400 μbar, and decreased beyond 400 μbar. V_{cmax} and *Rd* estimated from M2s were similar to those estimated from M1s.

3.1.2. Effects of transition C_i on g_m

The effects of the transition C_i cut-off on the estimates of g_m were analyzed with various methods with the whole A/C_i data set from SoyFACE. The g_m values varied greatly with transition C_i and varied greatly from method to method (Fig. 2). There were several patterns for various methods. The first pattern included g_{m1}_M2s, which was the highest and held constant g_m (g_m = 30) across the transition C_i range from 200 to 450 μbar. The second pattern included g_{m2}_M2s, g_m_M2c and g_m_M4c, which increased with transition C_i up to 300 μbar and then reached plateau. The third pattern included g_{m1}_M4s, which was constant from C_i cut-off range from 200 to 350 μbar, then gradually increased with further increase in transition C_i. The fourth pattern included g_{m2}_M4s, which increased with transition C_i up to 300 μbar, then slightly decreased with further increases in transition C_i. The g_m values estimated by combined iteration methods were proximately in-between the g_m values estimated by Rubisco-limited photosynthesis and the g_m values estimated by RuBP-limited photosynthesis.

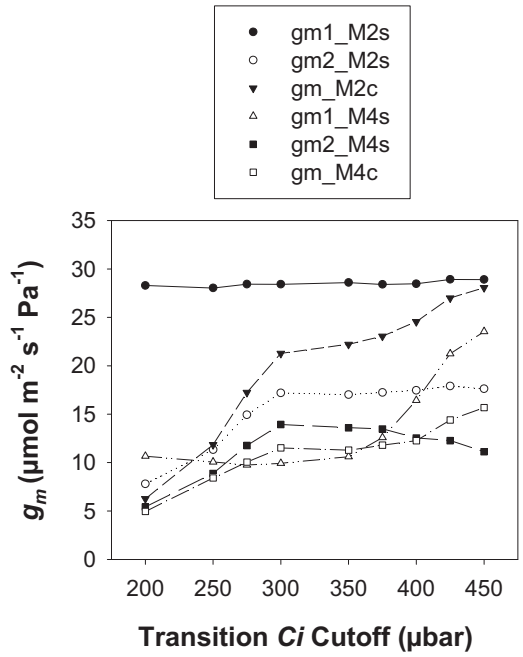

Fig. 2. Effects of transition C_i cut-off on mesophyll conductance (g_m) using various methods (● M1s, ○ M1c, ▼ M2s, ▽ M2c, ■ M4s and □ M4c). The estimates were the average across the whole set of data from SoyFACE.

3.2. Comparisons of various methods

3.2.1. Correlations among various methods

The correlations of V_{cmax}, J_{max} and *Rd* among various methods varied (Table 1). First, the correlations of M1c with M2c and M4c were surprisingly low for V_{cmax}, R^2 0.6094 and 0.3340, respectively.

Table 1
Correlations of V_{cmax}, J_{max} and *Rd* among various A/C_i curve fitting methods (*R* square).

	V_c_M1s	V_c_M2c	V_c_M2s	V_c_M4c	V_c_M4s
V_c_M1c	0.99927	0.60944	0.97891	0.33399	0.81225
V_c_M1s		0.60732	0.9787	0.32283	0.81374
V_c_M2c			0.6536	0.82238	0.53201
V_c_M2s				0.36089	0.8041
V_c_M4c					0.26751
	*J*_M1s	*J*_M2c	*J*_M2s	*J*_M4c	*J*_M4s
*J*_M1c	0.99505	0.98851	0.99298	0.97579	0.99003
*J*_M1s		0.98247	0.98665	0.96745	0.98681
*J*_M2c			0.99465	0.99245	0.99131
*J*_M2s				0.99123	0.99332
*J*_M4c					0.98611
	*Rd*_M1s	*Rd*_M2c	*Rd*_M2s	*Rd*_M4c	*Rd*_M4s
*Rd*_M1c	0.98967	0.76034	0.9683	0.66577	0.82094
*Rd*_M1s		0.7424	0.96628	0.62801	0.83357
*Rd*_M2c			0.81233	0.91187	0.65365
*Rd*_M2s				0.69854	0.83435
*Rd*_M4c					0.58706
	g_{m1}_M2s	g_{m2}_M2s	g_m_M4c	g_{m1}_M4s	g_{m2}_M4s
g_m_M2c	0.22076	0.84117	0.8533	0.04103	0.82643
g_{m1}_M2s		0.11814	0.16697	0.28643	0.11011
g_{m2}_M2s			0.87387	−0.03665	0.97583
g_m_M4c				0.05171	0.87733
g_{m1}_M4s					−0.08019
	C_{itr}_M2c	C_{itr}_M4c			
C_{itr}_M1c	0.4829	0.1406			
C_{itr}_M2c		0.4599			

Table 2
Probabilities (p-values) for ANOVA analysis of the effects of [CO_2] treatment, time (leaf age) and cultivar on V_{cmax}, Rd and J_{max} estimated by various A/C_i curve fitting methods.

	M1c	M1s	M2c	M2s	M4c	M4s
V_{cmax}						
Treatment	<0.0001	<0.0001	ns	<0.0001	0.0581	<0.0005
Time	<0.0001	<0.0001	0.0005	<0.0001	ns	<0.0001
Cultivar	ns	ns	ns	ns	ns	ns
Rd						
Treatment	ns	ns	ns	ns	0.0626	ns
Time	<0.0001	<0.0001	0.0721	<0.0001	ns	<0.0001
Cultivar	ns	ns	ns		ns	ns
J_{max}						
Treatment	ns	ns	ns	ns	ns	ns
Time	<0.0001	<0.0001	<0.0001	<0.0001	<0.0001	<0.0001
Cultivar	ns	ns	ns	ns	ns	ns
C_{itr}						
Treatment	<0.0001		0.0042		ns	
Time	<0.0001		ns		ns	
Cultivar	Ns		ns		ns	

ns, not significant. The interactions not listed were not significant.

Second, the correlations of V_{cmax} among various methods (R^2 between 0.2675 and 0.9993) were lower than the correlations of Rd among various methods (R^2 between 0.6658 and 0.9897), which, in turn, were lower than the correlations of J_{max} among various methods (R^2 between 0.9675 and 0.9951). Third, the correlations among the separated iteration methods (M1s, M2s and M4s, R^2 0.8041–0.9787) were higher than those among the combined iteration methods (M1c, M2c and M4c, R^2 0.3340–0.8224). Lastly, the correlations between the linear models (M1s and M1c) were higher than those between the rectangular models (M2s and M2c), which, in turn, were higher than those between the non-rectangular models (M4s and M4c). The correlations of V_{cmax}, J_{max} and Rd were 0.9993, 0.9951 and 0.9897, respectively, between M1s and M1c, were 0.6536, 0.9947 and 0.8123, respectively, between M2s and M2c, and were 0.2675, 0.9861 and 0.5871, respectively, between M4s and M4c.

3.2.2. Transition C_i (C_{itr})

C_{itr} values were not consistent among various methods (Fig. 3). On average, C_{itr} was significantly higher in M1c (395 μbar) than in M2c (340 μbar), which, in turn, was significantly higher than M4c (312 μbar). The effects of [CO_2] treatment and leaf aging on C_{itr} varied among methods (Table 2 and Fig. 3). Elevated [CO_2] significantly increased the C_{itr} for M1c and M2c, but not M4c. Leaf aging significantly increased the C_{itr} for M1c but not for M2c and M4c. For M1c, C_{itr} increased 24% under elevated [CO_2] versus ambient [CO_2] ($p < 0.001$), and increased 16% in R6 versus R5 ($p < 0.05$). There were significant interactions between treatment and time (Fig. 3). The difference of C_{itr} change between elevated [CO_2] versus ambient [CO_2] was higher in R6 stage than R5 stage, i.e. 32% and 15%, respectively. In addition, the difference of C_{itr} change between R6 and R5 was higher under elevated [CO_2] versus ambient [CO_2], i.e. 24% and 7%, respectively.

3.2.3. Maximum rate of Rubisco carboxylation (V_{cmax})

V_{cmax} values were not consistent among methods (Fig. 4 and Table 2). Elevated [CO_2] significantly decreased the V_{cmax} for all methods but M2c and M4c. V_{cmax}-M4c even increased rather than decreased under elevated [CO_2]. Leaf aging significantly decreased the V_{cmax} for all methods but M4c. The V_{cmax} values among the separated iterations (M1s, M2s and M4s) had better agreement than that among the combined iterations (M1c, M2c and M4c), which were consistent with the correlation of V_{cmax} among various methods (Table 1). V_{cmax} values estimated by non-rectangular models M4s and M4c were higher than other methods (Fig. 4 and Table 2). On average, V_{cmax} was 44% higher for the non-rectangular models and 13% higher for the rectangular models (M2s and M2c) compared with that for the linear models. The differences in V_{cmax} due to [CO_2] treatment were higher by the separated iteration methods (M4s and M2s) than the combined iteration methods (M4c and M2c).

3.2.4. Mitochondrial respiration rate in the light (Rd)

Mitochondrial respiration rate in the light (Rd) values were not consistent among methods (Fig. 4 and Table 2). Elevated [CO_2] did not significantly change the Rd for all methods but M4c. Leaf aging

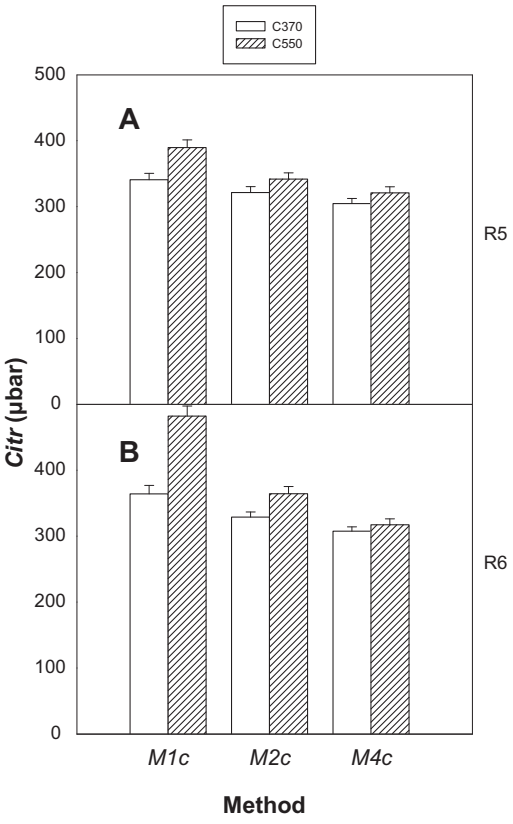

Fig. 3. C_{itr} calculated with various methods at R5 stage (A) and R6 stage (B). The leaves were sampled from plants grown at ambient [CO_2] of 370 μbar (open bar) or elevated [CO_2] of 550 μbar (hatched bar).

Table 3
Probabilities (p-values) of ANOVA analysis of the effects of [CO_2] treatment, time (leaf age) and cultivar on mesophyll conductance (g_m) estimated by various A/C_i curve fitting methods.

	Treatment	Time	Cultivar
g_m_M2c	0.0002	0.0109	ns
g_m_M4c	0.0043	0.057	ns
g_{m1}_M2s	0.0223	ns	ns
g_{m2}_M2s	0.0011	0.0107	ns
g_{m1}_M4s	0.0133	<0.0001	ns
g_{m2}_M4s	0.0004	0.0115	ns
g_m_VJ	ns	ns	ns
g_m_CJ	0.0927	0.1196	ns
g_m_Average	0.0708	0.035	ns

ns, not significant. The interactions not listed were not significant.

significantly decreased the *Rd* for all methods but M4c. The *Rd* values among the separated iterations (M1s, M2s and M4s) had better agreement than that among the combined iterations (M1c, M2c and M4c), which were consistent with the correlation of *Rd* among various methods (Table 1).

3.2.5. Maximum rate of electron transport (J_{max})

The J_{max} values were relatively consistent across various methods (Fig. 4 and Table 2). Of all the methods, J_{max} decreased in R6 versus R5 ($p < 0.001$), but was similar between [CO_2] treatments. Across all of the methods, J_{max} decreased from 161 in R5 to 135 in R6, i.e. decreased 20% in R6 versus R5.

3.2.6. Mesophyll conductance (g_m)

g_m was evaluated using both constant J (CJ) and variable J (VJ) methods (Fig. 5 and Table 3). g_m estimated by VJ was not significantly affected by either [CO_2] treatment or leaf aging. However, the effect of [CO_2] treatment on g_m estimated by CJ was significant ($p = 0.0927$). The effect of leaf aging on g_m estimated by CJ was close to significant. The g_m estimates were similar among the cultivars tested.

Mesophyll conductance (g_m) estimated using various curve-fitting methods varied (Fig. 5 and Table 3). First, g_{m2} that was estimated from RuBP-limited photosynthesis was significantly affected by [CO_2] treatment and leaf aging across all of the methods ($p < 0.05$), and had similar trends to the g_m estimated by CJ. Second, g_m estimated by combined iteration methods was in-between the g_{m1} and g_{m2} and was significantly affected by [CO_2] treatment and leaf aging. However, g_{m1} that was estimated from Rubisco-limited photosynthesis was not consistent with the g_{m2} values that estimated from RuBP-limited photosynthesis, and the g_m values estimated from VJ. Elevated [CO_2] significantly decreased the g_{m1} values for all of the methods except for VJ. g_{m1}_M4c even increased rather than decreased under elevated [CO_2].

The g_m values estimated by rectangular hyperbola curve fitting methods (M2c and M2s) were higher than those estimated by non-rectangular hyperbola curve fitting methods (M4c and M4s), which, in turn, were higher than those estimated by chlorophyll fluorescence (VJ and CJ). The g_m estimated using various curve-fitting methods did not appear to be within normal distribution. Many of the g_m values were at the maximum limit of 30.

In addition, g_m was found to be affected by instantaneous changes in [CO_2] (Fig. 6). C_i set the limit for maximum g_m. Log(g_m) was negatively correlated with C_i levels ($R = 0.5384$, $p < 0.01$).

3.3. Evaluation of V_{cmax}, J_{max}, Rd and g_m using combined chlorophyll fluorescence with gas exchange

Since V_{cmax}, J_{max} and *Rd* were not consistent among the various methods, we wonder which one was most likely true. To test this, the A/C_i curves were converted into A/C_c curves using the average g_m estimated by the constant J method and variable J method using chlorophyll fluorescence, and were re-analyzed by

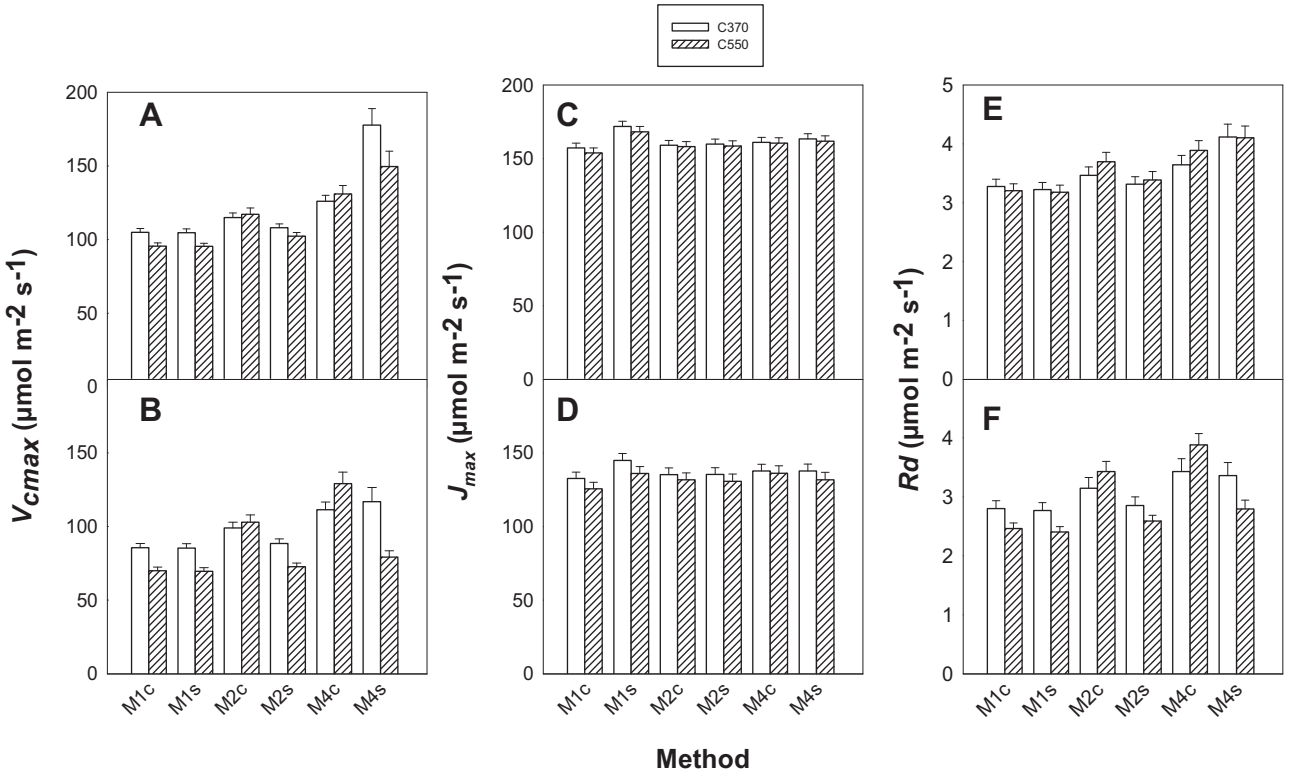

Fig. 4. V_{cmax}, J_{max} and *Rd* estimated by various curve fitting methods at R5 stage (A, C and E) and R6 stage (B, D and F). The leaves were sampled from plants grown at ambient [CO_2] of 370 μbar (open bar) or elevated [CO_2] of 550 μbar (hatched bar).

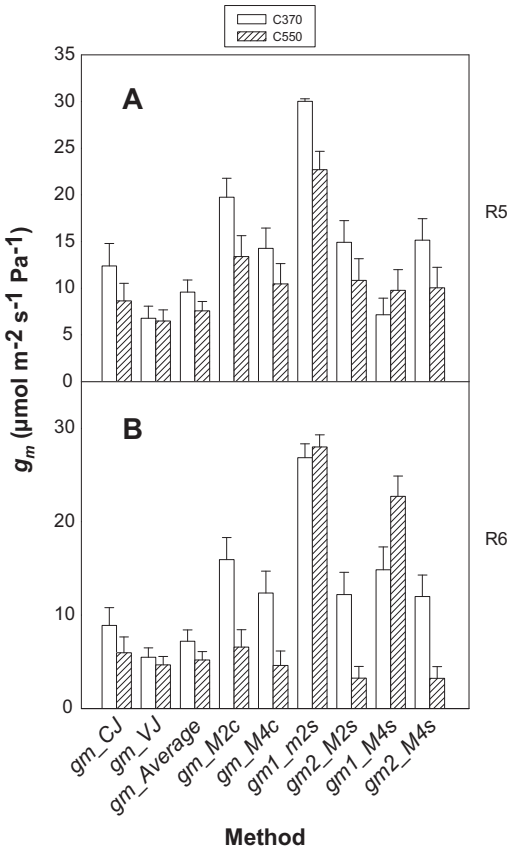

Fig. 5. Mesophyll conductance (g_m) estimated by various methods at R5 stage (A) and R6 stage (B). The leaves were sampled from plants grown at ambient [CO_2] of 370 μbar (open bar) or elevated [CO_2] of 550 μbar (hatched bar). CJ, constant *J* method, VJ, variable *J* method, g_m_Average, g_m average of CJ and VJ.

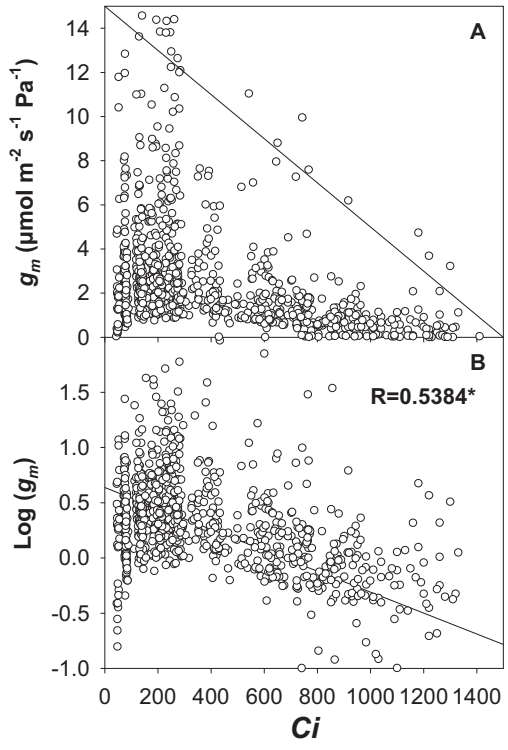

Fig. 6. The relationship between C_i and mesophyll conductance (g_m) estimated using variable *J* method.

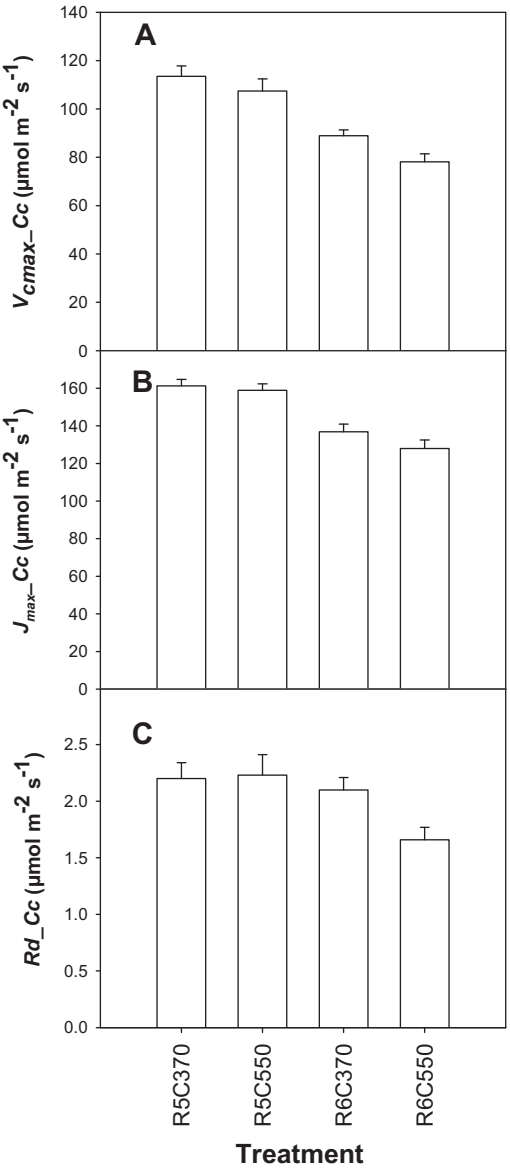

Fig. 7. V_{cmax} (A), J_{max} (B) and *Rd* (C) estimated from least square fitting A/C_c curves converted from A/C_i curves using average g_m from constant *J* and variable *J* methods at various treatment combinations of developmental stages (R5 or R6) and [CO_2] treatments (C370, 370 μbar [CO_2] or C550, 550 μbar [CO_2]).

linear models M1c (Fig. 7). V_{cmax}_C_c was consistent with V_{cmax}_M1c and remained significantly different between [CO_2] treatments ($p < 0.01$) and development stages ($p < 0.0001$). When g_m limitation was removed, V_{cmax} would increase 18%, whereas J_{max} would be essentially not changed. V_{cmax}_C_c decreased 10% in elevated [CO_2] versus ambient [CO_2], and decreased 25% in R6 versus R5. The decrease in V_{cmax} under [CO_2] enrichment was greater in R6 than in R5. [CO_2] enrichment decreased V_{cmax} 5.4% and 12.1% in R5 and R6, respectively. J_{max} decreased 17% in R6 versus R5 ($p < 0.001$), but was similar between [CO_2] treatments.

Since g_m changed with instantaneous change in [CO_2] (Fig. 6), the A/C_c curves were also converted from A/C_i curves using the g_m estimated at individual C_i by variable *J* method, and were re-analyzed by M1c. V_{cmax}_C_c estimated this way was similar to that using the average g_m estimated from variable *J* and constant *J* methods (data not shown).

4. Discussion

4.1. The estimates of V_{cmax} and g_m are inconsistent among the various methods

Unexpectedly we found inconsistency among the various methods of linear, rectangular and non-rectangular hyperbola models for the estimates of V_{cmax} and g_m using combined least square fitting of the A/C_i curves. First, the correlations of the linear model M1c with the rectangular hyperbola model M2c and the non-rectangular model M4c were surprisingly low, R^2 0.6094 and 0.3340, respectively. Second, the estimates and patterns of V_{cmax} and g_m were different among various methods (Figs. 4, 5 and 7). Third, the effects of elevated [CO_2] and leaf aging on the estimates of V_{cmax} and g_m were not consistent among various methods (Tables 2 and 3). Thus different conclusions might be made. It might be concluded that either elevated [CO_2] or leaf aging would significantly down-regulate V_{cmax} but not g_m based on the results from M1c and variable J method, whereas, it might also be concluded that either elevated [CO_2] or leaf aging would significantly down-regulate g_m but not V_{cmax} based on the results from M2c and M4c (Figs. 4, 5 and 7). Both V_{cmax} and g_m influence the leaf photosynthetic capacity. M2c and M4c methods basically enlarged the effects of elevated [CO_2] or leaf aging on g_m while reduced the effects of elevated [CO_2] or leaf aging on V_{cmax} compared with M1c and variable J methods.

There was a report in which some of the curve-fitting methods were compared [12]. Unfortunately, a constant 20 Pa [CO_2] was used as the transition C_i cut-off for many of the methods of comparisons and M1 method was not included [12]. Thus it is difficult to determine which method makes sense and which factors are the causes for the differences among the methods. The assumption that the C_i value at which the A/C_i curve switches between Rubisco- and RuBP-regeneration-limited portions of the curve (C_i–t) is set to a constant would influenced the accuracy of parameter estimation. It showed the C_{itr} value varied significantly, ranging from 24 Pa to 72 Pa and averaging 38 Pa. We use the computing programs to automatically determine C_{itr} using least square fitting of each of the A/C_i curves and thus can actually compare these methods to find out whether the estimates from these methods are consistent and which factors are the likely causes for the inconsistency. Our results clearly showed that the estimates from various methods are not consistent when using combined least square fitting.

4.2. The inconsistency among the various methods is due to the changes of g_m with C_i and the sensitivity to transition C_i cut-off

Mesophyll conductance estimated from combined chlorophyll fluorescence with gas exchange indicated that g_m was not constant and decreased with increase in C_i using variable J methods (Fig. 6), which was in agreement with the previous reports [15,23–25]. Recent studies demonstrated a rapid change in g_m with other instantaneous environmental changes such as temperature, light intensity and water loss similar as stomatal conductance [25]. Mesophyll conductance is also affected by photorespiration [21]. The dynamic g_m changes with environmental conditions are not well understood. It is generally assumed that g_m is constant throughout the measurements of A/C_i curves [7,8,11,13,14,21]. Since g_m and Rd are present in both Rubisco- and RuBP-limited photosynthesis, the combined iterations of both Rubisco-limited and RuBP-limited photosynthesis would increase in the number of measurements for estimates of g_m and Rd. There is no evidence that Rd is different between Rubisco-limited and RuBP-limited photosynthesis. Therefore a unique value for g_m and Rd can be obtained by combined iterations of both Rubisco-limited and RuBP-limited photosynthesis.

Table 4
Correlations of V_{cmax}, J_{max} and Rd among various A/C_i curve fitting methods (R square) by applying C_{itr} calculated from M1c to all of the methods.

	M1s	M2c	M2s	M4c	M4s
V_{cmax}					
M1c	0.9991	0.8904	0.9987	0.5201	0.8074
M1s		0.8830	0.9994	0.5064	0.8070
M2c			0.8856	0.6742	0.7311
M2s				0.5056	0.8143
M4c					0.4434
J_{max}					
M1c	0.9996	0.9966	0.9999	0.9800	0.9775
M1s		0.9953	0.9996	0.9774	0.9742
M2c			0.9966	0.9852	0.9790
M2s				0.9800	0.9775
M4c					0.9779
Rd					
M1c	0.9714	0.9693	0.9732	0.7993	0.9091
M1s		0.9256	0.9932	0.7508	0.9260
M2c			0.9333	0.8429	0.8808
M2s				0.7660	0.9436
M4c					0.7388

Mesophyll conductance varied with transition C_i cut-off and varied from method to method (Fig. 2). Mesophyll conductance was lower when using smaller transition C_i cut-off than when using larger transition C_i cut-off. Finding the right transition C_i cut-off is critical for A/C_i curve fitting. In many reports, a constant transition C_i was assigned by looking at the A/C_i curves and/or based on the literature information. This may cause problems since various species and treatments may have different transition C_i (Fig. 3). A constant transition C_i cut-off is not suitable especially for the rectangular and non-rectangular hyperbola models since these models are even more sensitive to transition C_i cut-off. In this study we have developed the Excel macro and SAS code that can automatically determine C_{itr} using least-square fitting with minimum RMSE, and automatically process multiple data sets of A/C_i curves, thus making the analysis much easier and more consistent. There are good correlations for the estimates between Excel macro and SAS code (Fig. 10).

Addition of one more variable, g_m, would increase one more degree of freedom and decrease the power of iterations. It was found that the pre-set value and range limit of g_m had significant effects on the iterations for the hyperbola models (data not shown). While the g_m values estimated by the combined chlorophyll fluorescence with gas exchange (variable J method) is basically of normal distribution, the g_m values estimated by curve-fitting is not of normal distribution with many g_m values at or near the pre-set maximum limit. We wonder whether the lower C_{itr} estimated from M2 and M4 caused the different conclusions compared with that from M1 and that from the combined chlorophyll fluorescence with gas exchange. C_{itr} was significantly higher in M1c (395 μbar) than in M2c (340 μbar), which, in turn, was significantly higher than M4c (312 μbar) (Fig. 3). It is opposite to what it is expected. Logically, C_{itr} should increase instead of decrease in order to keep up with the CO_2 requirement at Rubisco if g_m is low.

Consistency in estimates of V_{cmax} may be improved by fixing one or more parameters (*e.g.* Rd and/or J_{max}) and by using the generic models [24,26,27], which usually requires additional measurements such as chlorophyll fluorescence and/or gas exchange under several light levels and/or oxygen levels or other assumptions such as empirical relationships between potential electron transport (J) and light. It was found that better consistency was achieved by applying C_{itr} estimated from M1c to all of the methods (Fig. 8 and Table 5). The correlations among various methods were better when the C_{itr} values estimated from M1c were applied to all of the methods (Table 4) compared with the previous ones using

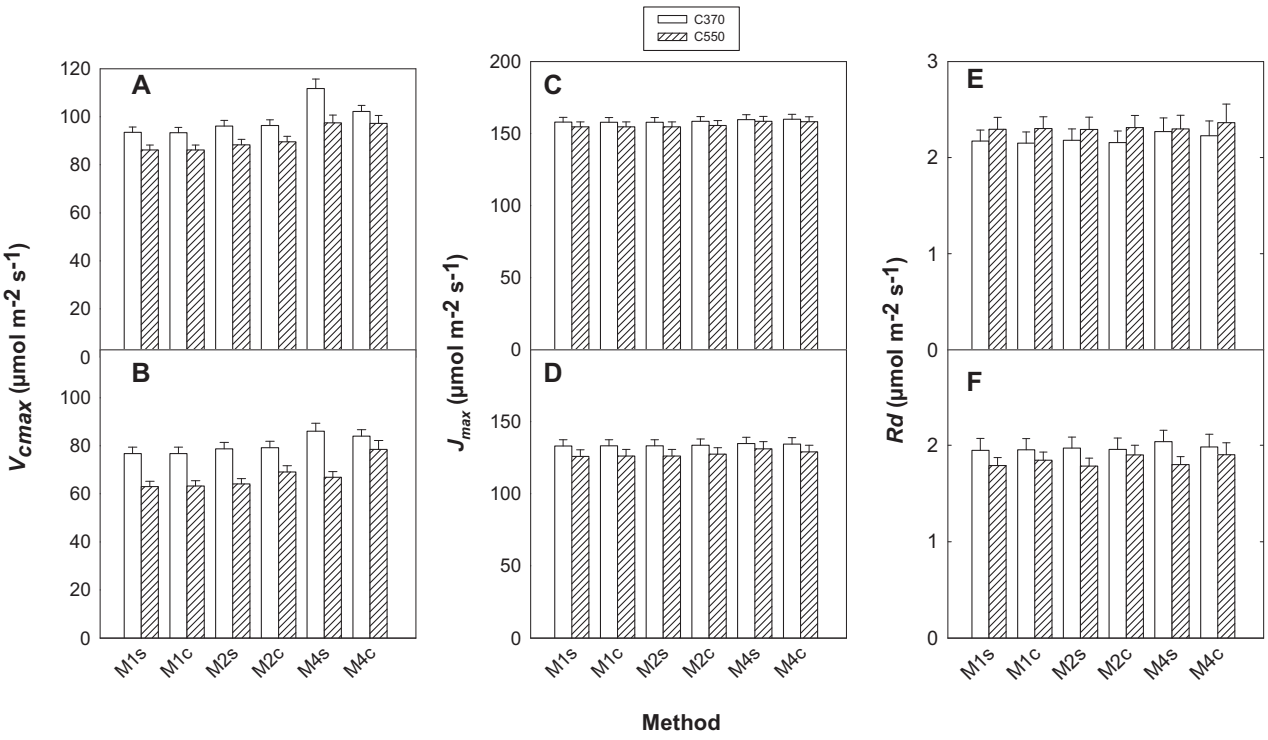

Fig. 8. V_{cmax}, J_{max} and *Rd* estimated by various curve fitting methods using C_{itr} calculated by M1c instead at R5 stage (A, C and E) and R6 stage (B, D and F). The leaves were sampled from plants grown at ambient [CO_2] of 370 μbar (open bar) or elevated [CO_2] of 550 μbar (hatched bar).

Table 5
Probabilities (*p*-values) for ANOVA analysis of the effects of [CO_2] treatment, time (leaf age) and cultivar on V_{cmax}, *Rd* and J_{max} estimated by various A/C_i curve fitting methods by applying C_{itr} calculated from M1c to all of the methods.

	M1s	M1c	M2s	M2c	M4s	M4c
V_{cmax}						
Treatment	<0.0001	<0.0001	<0.0001	0.0007	<0.0001	<0.0720
Time	<0.0001	<0.0001	<0.0001	<0.0001	<0.0001	<0.0001
Cultivar	ns	ns	ns	ns	ns	ns
Rd						
Treatment	ns	ns	ns	ns	ns	ns
Time	0.0018	0.0040	0.0020	0.0103	0.0045	0.0235
Cultivar	ns	ns	ns		ns	ns
J_{max}						
Treatment	ns	ns	ns	ns	ns	ns
Time	<0.0001	<0.0001	<0.0001	<0.0001	<0.0001	<0.0001
Cultivar	ns	ns	ns	ns	ns	ns

ns, not significant. The interactions not listed were not significant.

different C_{itr} (Table 1). Better consistency was also achieved by separated iterations of either the Rubisco-limited photosynthesis or RuBP-limited photosynthesis (Figs. 8 and 9 and Tables 5 and 6). To test whether these approaches should be trusted, the A/C_i curves were converted into A/C_c curves using the g_m estimated by combined chlorophyll fluorescence with gas exchange, and were re-analyzed by linear models M1c (Fig. 7). V_{cmax}_C_c was consistent with V_{cmax}_*M1c* and remained significantly different between [CO_2] treatments and development stage. When g_m limitation was removed, V_{cmax} would increase by 18%. The theories for the possible approach applying C_{itr} estimated from M1c to other type of curve-fitting may need further studies in the future.

Table 6
Probabilities (*p*-values) for ANOVA analysis of the effects of [CO_2] treatment, time (leaf age) and cultivar on mesophyll conductance (g_m) estimated by various A/C_i curve fitting methods by applying C_{itr} calculated from M1c to all of the methods.

	Treatment	Time	Cultivar
g_m_M2c	0.01250	0.0077	ns
g_m_M4c	<0.0001	0.1149	ns
g_{m1}_M2s	ns	ns	ns
g_{m2}_M2s	<0.0001	<0.0001	ns
g_{m1}_M4s	ns	ns	ns
g_{m2}_M4s	0.0005	0.0126	ns

4.3. Elevated [CO_2] and leaf aging down-regulates V_{cmax}

Long-term elevated [CO_2] resulted in the reduction of photosynthetic capacity. The maximum rates of Rubisco carboxylation (V_{cmax}) calculated from A/C_c curves decreased 10% in elevated [CO_2] versus ambient [CO_2] (Fig. 7), indicating down-regulation of Rubisco. The reduction in V_{cmax} by elevated [CO_2] is similar to the previous reports [28,29]. The close correlation is demonstrated between V_{cmax} estimated by gas exchange and V_{cmax} estimated from maximum Rubisco activity [29]. There is abundant evidence that Rubisco is down regulated under [CO_2] enrichment.

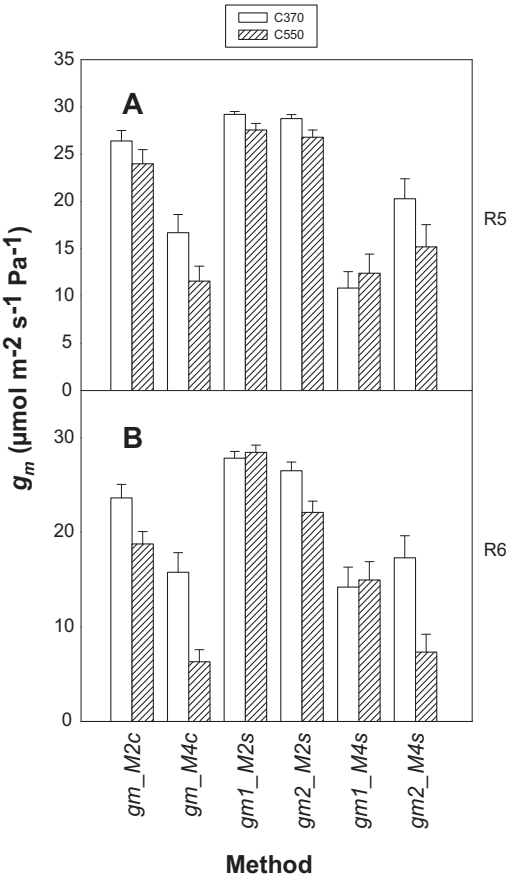

Fig. 9. Mesophyll conductance (g_m) estimated by various methods using C_{itr} calculated by M1c instead at R5 stage (A) and R6 stage (B). The leaves were sampled from plants grown at ambient [CO_2] of 370 μbar (open bar) or elevated [CO_2] of 550 μbar (hatched bar). CJ, constant *J* method, VJ, variable *J* method, g_m_Average, g_m average of CJ and VJ.

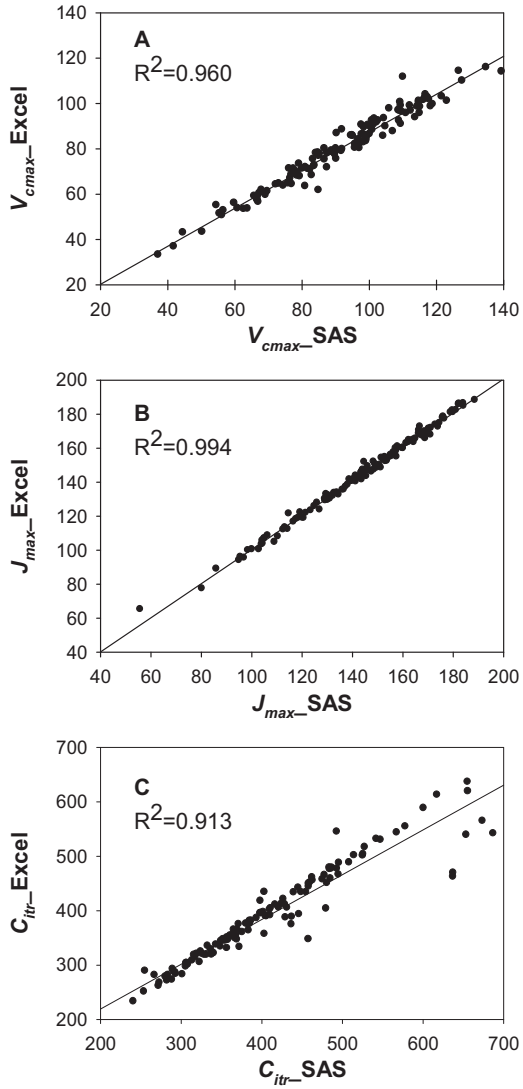

Fig. 10. The correlations of V_{cmax} (A), J_{max} (B) and C_{itr} (C) between the estimates from the M1c method with SAS code and the estimates from M1c method with Excel solver.

Down-regulation of Rubisco small subunit (*rbcS*) transcripts is reported in many plant species [*e.g.* 30–32]. This correlates with a decrease in Rubisco activity [31,32] and/or content [30]. In *Arabidopsis* both Rubisco protein and Rubisco activation decreased under elevated [CO_2] compared with ambient [CO_2] [33]. The meta-analysis shows 13% reduction of Rubisco protein across FACE experiments [1]. Carbohydrate accumulation in leaves under elevated [CO_2] could be the reasons for down-regulation of Rubisco. Measurements of photosynthesis and foliar carbohydrate content showed that plants growing at elevated [CO_2] had a 25% increase in the daily integral of photosynthesis and 58% increase in leaf carbohydrate content [2,34]. The increased accumulation of soluble sugars is correlated with a reduction of *rbcs* expression through so-called sugar-sensing [30–32,35].

Mesophyll conductance affects the V_{cmax} estimate when g_m is not infinite and imposes significant limitation on photosynthesis (Fig. 7). V_{cmax} would be underestimated if g_m is small. When g_m limitation is removed V_{cmax} increases 18% (Figs. 7 and 8), which is consistent with the reported 10–20% limitation by g_m [19]. Mesophyll conductance estimated by the constant *J* method (g_m_CJ) was significantly affected by elevated [CO_2], but g_m estimated by the variable *J* method (g_m_VJ) was not (Table 3). This explains the differences in the effects of elevated [CO_2] on g_m in the previous reports since the constant *J* method was used for one report [28] and the variable *J* method was used for another report [36].

V_{cmax} also decreased due to leaf aging. V_{cmax} decreased by 22% in R6 versus R5 with various methods (Fig. 7). Similar to CO_2 enrichment effect, g_m differences due to leaf aging were only observed under RuBP-limited photosynthesis, but not under Rubisco-limited photosynthesis (Table 6 and Fig. 9). Under RuBP-limited photosynthesis, photosynthesis is less likely limited by [CO_2]. Reports on the effects of leaf aging on photosynthetic biochemistry are not consistent among studies. In Arabidopsis a 40% decrease in photosynthesis of 45-day-old versus 30-day-old leaves was entirely caused by increased diffusional limitations to CO_2 transfer, of which decreased mesophyll conductance was the largest as shown by a quantitative limitation analysis [15]. On the other hand, the age-related reduction of photosynthesis is assumed to be mainly due to the degradation of chlorophylls, Rubisco and other chloroplast proteins and g_m contribution is minor [37]. It was suggested that the age-related decline in photosynthesis in wheat may be attributed in part to a reduction in g_m and in part to a decline in the amount of Rubisco [38]. In addition to the species differences, different methods used for the estimates may likely be part of the reasons for the differences.

5. Conclusions

There is inconsistency among the various A/C_i curve-fitting methods for the estimates of C_{itr}, V_{cmax}, Rd and g_m which may lead to

different conclusions as which would be affected, V_{cmax} or g_m. The inconsistency is due to the inconsistent estimates of g_m values that varies with transition C_i cut-off and due to over-parameters in the non-linear methods in which g_m is included for A/C_i curve-fitting. We do not intend to invalidate the non-linear methods, rather to let people aware of the limitations. An alternate solution to A/C_i curve-fitting for estimates of V_{cmax} and g_m is proposed. The limitation of photosynthetic capacity by g_m is 18% on average. Analysis of the SoyFACE data by various methods indicates that down-regulation of photosynthetic capacity by elevated [CO_2] and leaf aging is partially due to the decrease in the maximum rates of carboxylation (V_{cmax}, i.e. decreased carboxylation conductance) and partially due to the decrease in g_m for soybean plants grown under elevated CO_2.

Appendix A. Supplementary data

Supplementary data associated with this article can be found, in the online version, at http://dx.doi.org/10.1016/j.plantsci.2014.06.015.

References

[1] E.A. Aintworth, S.P. Long, What have we learned from 15 years of free-CO_2 enrichment (FACE)? A meta-analytic review of the responses of photosynthesis, canopy properties and plant production to rising CO_2, New Phytol. 165 (2005) 351–372.

[2] J. Sun, L.-X. Yang, Y.-L. Wang, D.R. Ort, Review: FACE-ing the global change: new opportunities for crop improvement in photosynthetic radiation use efficiency and crop yield, Plant Sci. 177 (2009) 511–522.

[3] G.D. Farquhar, S. von Caemmerer, J.A. Berry, A biochemical model of photosynthetic CO_2 assimilation in leaves of C3 species, Planta 149 (1980) 78–90.

[4] S. von Caemmerer, G.D. Farquhar, Some relationships between the biochemistry of photosynthesis and the gas exchange of leaves, Planta 153 (1981) 376–387.

[5] P.C. Harley, T.D. Sharkey, An improved model of C3 photosynthesis at high CO_2: reversed O_2 sensitivity explained by lack of glycerate reentry into the chloroplast, Photosynth. Res. 27 (1991) 169–178.

[6] S. von Caemmerer, Biochemical Models of Leaf Photosynthesis, CSIRO Publishing, Collingwood, Victoria, Australia, 2000, pp. 1–165.

[7] P.C. Harley, F. Loreto, G. DiMarco, T.D. Sharkey, Theoretical considerations when estimating the mesophyll conductance to CO_2 flux by analysis of the response of photosynthesis to CO_2, Plant Physiol. 98 (1992) 1429–1436.

[8] F. Loreto, P.C. Harley, G. DiMarco, T.D. Sharkey, Estimation of mesophyll conductance to CO_2 flux by three different methods, Plant Physiol. 98 (1992) 1437–1443.

[9] S.P. Long, C.J. Bernacchi, Gas exchange measurements, what can they tell us about the underlying limitations to photosynthesis? Procedures and sources of error, J. Exp. Bot. 54 (2003) 2393–2401.

[10] J.B. Dubois, E.L. Fiscus, F.L. Booker, M.D. Flowers, C.D. Reid, Optimizing the statistical estimation of the parameters of the Farquhar–von Caemmerer–Berry model of photosynthesis, New Phytol. 176 (2007) 402–414.

[11] T.D. Sharkey, C.J. Bernacchi, G.D. Farquhar, E.L. Singsaas, Fitting photosynthetic carbon dioxide response curves for C3 leaves, Plant Cell Environ. 30 (2007) 1035–1040.

[12] Z. Miao, M. Xu, R.G. Lathrop, J.R.Y. Wang, Comparison of the A–C_c curve fitting methods in determining maximum ribulose 1,5-bisphosphate carboxylase/oxygenase carboxylation rate, potential light saturated electron transport rate and leaf dark respiration, Plant Cell Environ. 32 (2009) 109–122.

[13] G.J. Ethier, N.J. Livingston, On the need to incorporate sensitivity to CO_2 transfer conductance into the Farquhar–von Caemmerer–Berry leaf photosynthesis model, Plant Cell Environ. 27 (2004) 137–153.

[14] G.J. Ethier, N.J. Livingston, D.L. Harrison, T.A. Black, J.A. Moran, Low stomatal and internal conductance to CO_2 versus Rubisco deactivation as determinants of the photosynthetic decline of ageing evergreen leaves, Plant Cell Environ. 29 (2006) 2168–2184.

[15] J. Flexas, M.F. Ortuño, M. Ribas-Carbo, A. Diaz-Espejo, I.D. Flórez-Sarasa, H. Medrano, Mesophyll conductance to CO_2 in *Arabidopsis thaliana*, New Phytologist 175 (2007) 501–511.

[16] J.R. Evans, T.D. Sharkey, J.A. Berry, G.D. Farquhar, Carbon isotope discrimination measured concurrently with gas exchange to investigate CO_2 diffusion in leaves of higher plants, Aust. J. Plant Physiol. 13 (1986) 281–292.

[17] B. Genty, J. Briantais, N.R. Baker, The relationship between the quantum yield of photosynthetic electron transport and quenching of chlorophyll fluorescence, Biochim. Biophys. Acta 990 (1989) 87–92.

[18] E. Ogren, J.R. Evans, Photosynthetic light–response curves. I: The influence of CO_2 partial pressure and leaf inversion, Planta 189 (1993) 180–190.

[19] C.J. Bernacchi, A.R. Portis, H. Nakano, S. von Caemmerer, S.P. Long, Temperature response of mesophyll conductance. Implications for the determination of Rubisco enzyme kinetics and for limitations to photosynthesis in vivo, Plant Physiol. 130 (2002) 1992–1998.

[20] C.J. Bernacchi, E.L. Singsaas, C. Pimentel, A.R. Portis Jr., S.P. Long, Improved temperature response functions for models of Rubisco-limited photosynthesis, Plant Cell Environ. 24 (2001) 253–259.

[21] D. Tholen, G. Ethier, B. Genty, S. Pepin, X.-G. Zhu, Variable mesophyll conductance revisited: theoretical background and experimental implications, Plant Cell Environ. 35 (2012) 2087–2103.

[22] L. Gu, Y. Sun, Artefactual responses of mesophyll conductance to CO_2 and irradiance estimated with the variable J and online isotope discrimination methods, Plant Cell Environ. 37 (2013) 1231–1249.

[23] J. Flexas, A. Díaz-Espejo, J. Galmés, R. Kaldenhoff, H. Medrano, M. Ribas-Carbó, Rapid variations of mesophyll conductance in response to changes in CO_2 concentration around leaves, Plant Cell Environ. 30 (2007) 1284–1298.

[24] X. Yin, P.C. Struik, P. Romero, J. Harbinson, J.B. Evers, P.E.L. Van Der Putten, J. Vos, Using combined measurements of gas exchange and chlorophyll fluorescence to estimate parameters of a biochemical C-3 photosynthesis model: a critical appraisal and a new integrated approach applied to leaves in a wheat (*Triticum aestivum*) canopy, Plant Cell Environ. 32 (2009) 448–464.

[25] J. Flexas, M. Ribas-Carbo, A. Díaz-Espejo, J. Galmés, H. Medrano, Mesophyll conductance to CO_2: current knowledge and future prospects, Plant Cell Environ. 31 (2008) 602–621.

[26] L.-H. Gu, S.G. Pallardy, K. Tu, B.E. Law, S.D. Wullschleger, Reliable estimation of biochemical parameters from C3 leaf photosynthesis–intercellular carbon dioxide response curves, Plant Cell Environ. 33 (2010) 1853–1874.

[27] W. Zeng, G. Zhou, B. Jia, Y. Jiang, Y. Wang, Comparison of parameters estimated from A/C_i and A/C_c curve analysis, Photosynthetica 48 (3) (2010) 323–331.

[28] P.C. Harley, R.B. Thomas, J.F. Reynolds, B.R. Strain, Modelling photosynthesis of cotton grown in elevated CO_2, Plant Cell Environ. 15 (1992) 271–282.

[29] E.L. Singsaas, D.R. Ort, E.H. Delucia, Elevated CO_2 effects on mesophyll conductance and its consequences for interpreting photosynthetic physiology, Plant Cell Environ. 27 (2003) 41–50.

[30] S.-H. Cheng, B.D. Moore, J.R. Seemann, Effects of short- and long-term elevated CO_2 on the expression of ribulose-1,5-bisphosphate carboxylase/oxygenase genes and carbohydrate accumulation in leaves of *Arabidopsis thaliana*, Plant Physiol. 116 (1998) 715–723.

[31] N. Majeau, J.R. Coleman, Effect of CO_2 concentration on carbonic anhydrase and ribulose-1,5-bisphosphate carboxylase/oxygenase expression in pea, Plant Physiol. 112 (1996) 569–574.

[32] J.-J. Van Oosten, R.T. Besford, Some relationships between the gas exchange, biochemistry and molecular biology of photosynthesis during leaf development of tomato plants after transfer to different carbon dioxide concentrations, Plant Cell Environ. 18 (1995) 1253–1266.

[33] J. Sun, K.M. Gibson, O. Kiirats, T.W. Okita, G.E. Edwards, Interactions of nitrate and CO_2 enrichment on growth, carbohydrates, and rubisco in Arabidopsis starch mutants. Significance of starch and hexose, Plant Physiol. 130 (2002) 1573–1583.

[34] A. Rogers, Y. Gibon, M. Stitt, P.B. Morgan, C.J. Bernacchi, D.R. Ort, S.P. Long, Increased C availability at elevated carbon dioxide concentration improves N assimilation in a legume, Plant Cell Environ. 29 (2006) 1651–1658.

[35] J.-C. Jang, J. Sheen, Sugar sensing in higher plants, Plant Cell 6 (1994) 1665–1679.

[36] C.J. Bernacchi, P.B. Morgan, D.R. Ort, S.P. Long, The growth of soybean under free air [CO_2] enrichment (FACE) stimulates photosynthesis while decreasing in vivo Rubisco capacity, Planta 220 (2005) 434–446.

[37] J.W. Friedrich, R.C. Huffaker, Photosynthesis, leaf resistance, and ribulose-1,5-bisphosphate carboxylase degradation in senescing barley leaves, Plant Physiol. 65 (1980) 1103–1107.

[38] F. Loreto, G. Di Marco, D. Tricoli, T.D. Sharkey, Measurements of mesophyll conductance, photosynthetic electron transport and alternative electron sinks of field grown wheat leaves, Photosynth. Res. 41 (1994) 397–403.